IOP Publishing Quantum Sci. Technol. 10 (2025) 035019 https://doi.org/10.1088/2058-9565/add55d

Quantum Science and Technology

OPEN ACCESS

RECEIVED
8 January 2025

REVISED
10 April 2025

ACCEPTED FOR PUBLICATION
7 May 2025

PUBLISHED
15 May 2025

PAPER

Quantum speed limit for Kirkwood–Dirac quasiprobabilities

Sagar Silva Pratapsi[1,2,3,*], **Sebastian Deffner**[4,5,6] and **Stefano Gherardini**[7,8]

[1] CFisUC, Department of Physics, University of Coimbra, P-3004-516 Coimbra, Portugal
[2] Instituto Superior Técnico, University of Lisbon, 1049-001 Lisbon, Portugal
[3] Instituto de Telecomunicações, 1049-001 Lisbon, Portugal
[4] Department of Physics, University of Maryland, Baltimore County, Baltimore, MD 21250, United States of America
[5] Quantum Science Institute, University of Maryland, Baltimore County, Baltimore, MD 21250, United States of America
[6] National Quantum Laboratory, College Park, MD 20740, United States of America
[7] Istituto Nazionale di Ottica del Consiglio Nazionale delle Ricerche (CNR-INO), Largo Enrico Fermi 6, I-50125 Firenze, Italy
[8] European Laboratory for Non-linear Spectroscopy, Università di Firenze, I-50019 Sesto Fiorentino, Italy
[*] Author to whom any correspondence should be addressed.

E-mail: spratapsi@uc.pt, deffner@umbc.edu and stefano.gherardini@ino.cnr.it

Keywords: quantum, Kirkwood–Dirac, quasiprobabilities, quantum speed limit

Abstract

What is the minimal time until a quantum system undergoing unitary dynamics can exhibit genuine quantum features? To answer this question we derive quantum speed limits (QSLs) for two-time correlation functions arising from statistics of measurements. These two-time correlators are described by Kirkwood–Dirac quasiprobabilities, if the initial quantum state of the system does not commute with the measurement observables. The QSLs here introduced are derived from the Schrödinger–Robertson uncertainty relation, and set the minimal time at which the real part of a quasiprobability can become negative and the corresponding imaginary part can be different from zero or crosses a given threshold. This departure of Kirkwood–Dirac quasiprobabilities from positivity is evidence for the onset of non-classical traits in the quantum dynamics. As an illustrative example, we apply these results to a conditional quantum gate by determining the optimal condition that gives rise to non-classicality at maximum speed. In this way, our analysis hints at boosted power extraction due to genuinely non-classical dynamics.

The question asking whether a quantum process is truly quantum looks as innocuous, as it is deep. While many sophisticated answers could be given, such as referring to violations of Bell [1] or Leggett–Garg [2] inequalities, the simplest answer is arguably found in the presence of non-classical correlations [3].

In this paper, we focus on exactly such correlations that characterize the statistics of measuring two distinct quantum observables A and B, at the beginning and end of a unitary process with a non-negligible duration. Such two-time correlation functions [4] have become ubiquitous in modern physics, ranging from condensed matter physics and quantum chaos [5–13] to quantum thermodynamics [14–22]. Most quantum correlation functions can be computed even when the exact quantum state is not directly measurable [23–25].

Here we are interested in understanding if any universal statement can be made about the dynamics of such correlators. In fact, their time-evolution, like the dynamics of the system itself, are entirely generated by the Hamiltonian of the system. Hence, it appears obvious to consider *quantum speed limits* (QSLs) for correlation functions [26][9]. QSLs [27] set constraints on the maximum speed of the quantum evolution [28, 29]. From the seminal work of Mandelstam and Tamm [30, 31], it is known that the quantum speed is tightly bound by the Schrödinger–Robertson (SR) uncertainty relation [32, 33]. This gives the QSLs a fundamental connotation that links the minimal time to attain a quantum state transformation to the energy dispersion imposed by the system Hamiltonian. Obviously, correlation functions constructed from the statistics of measurement outcomes, recorded by measuring A and B, have to respect similar time constraints.

[9] Evidently, such limits are no longer useful if the observables A and B are measured consecutively without letting the system evolve.

In the present analysis, we focus on situations in which the initial quantum state does not commute with the measurement observables. In this non-commutative case, correlation functions are the *Kirkwood–Dirac quasiprobabilities* (KDQ) [25, 34–40], which in general are complex numbers whose real part can be also negative. The presence of negative real parts and of imaginary parts different from zero does not allow for building up a single joint distribution of events at multiple times according to classical probability theory [25, 40–42]. In particular, negativity has been interpreted as a meaningful trait of *non-classicality* [43], given that negative quasiprobabilities, as well as anomalous weak values, are a witness of quantum contextuality [44–50], as experimentally confirmed in [51–53]. Beyond its fundamental relevance, negativity has recently found experimental application to enhance both phase estimation [54] and work extraction [20], beyond classical limits. In addition, [55] introduces an interferometric procedure to reconstruct the imaginary parts of two-time KDQ distributions, thus giving access to non-commutativity.

In this work, we address the following questions: 'Can we predict the time at which a two-time correlator, in terms of KDQ, can become non-positive? And, can we take an advantage of such a prediction in a quantum technology application?' As main results, we demonstrate that the QSL predicts the *minimal time* for the emergence of non-positive KDQ, while measuring two non-commuting observables at distinct times. This goes beyond the QSL for the average of a single observable [28, 56], and finds application in the interdisciplinary field of evaluating the energetics of quantum computing gates [57–67], as well as quantum synchronization [68]. Moreover, the fact that the probability associated with a measurement-outcome pair is described by a non-positive KDQ outlines the role played by quantum coherence or correlations as a quantum resource. For instance, in non-equilibrium work processes our QSLs can be used to identify, and possibly reduce, the time corresponding to the largest enhancement of work extraction due to the negativity of the real part of some KDQ. Knowing such a time, which can be obtained without solving the system dynamics, allows to derive a tight bound on the work extraction power. We illustrate this for the two-qubit controlled-unitary gate of [60].

1. Kirkwood–Dirac quasiprobabilities

We start with notions and notations. Let ρ be a density operator, and A and B two distinct quantum observables (Hermitian operators), evaluated at times $t=0$ and $t>0$ respectively. The two observables have the spectral decompositions $A=\sum_\ell a_\ell A_\ell$ and $B=\sum_j b_j B_j$ with $A_\ell=A_\ell^2$ and $B_j=B_j^2$. In the present analysis, the evolution of the quantum system is described by a unitary operator $U\equiv\exp(-\mathrm{i}Ht/\hbar)$, where H denotes the system Hamiltonian, $\hbar$ is the reduced Planck constant and t the evolution time. In the following, we will also take into account the evolution of the quantum observable B, which is given by $B(t)\equiv U^\dagger BU$ in Heisenberg picture.

In general, KDQ are complex numbers and constitute a family of distributions of quasiprobabilities [40, 42]. For the purpose of this work, throughout the whole article, we take a representation of KDQ defined by two-time quantum correlators. In this regard, we can describe the statistics of the measurement-outcome pairs (a_ℓ,b_j), which occurs from evaluating the two quantum observables A and B at times $0,t$, with the KDQ

$$q_{\ell,j}(t)\equiv\mathrm{tr}\left\{\rho A_\ell B_j(t)\right\}, \tag{1}$$

where $B_j(t)=U^\dagger B_jU$ is the projector B_j evolved in the Heisenberg picture. In agreement with the no-go theorems of [25, 69], if the commutator of ρ and A is equal to zero ($[\rho,A]=0$), then the KDQ is a non-negative real number—as a standard probability obeying Kolmogorov axioms—and is given by the two-point measurement (TPM) scheme [70].

The statistics provided by the TPM scheme can be experimentally assessed by a procedure based on sequential measurements, as in the classical case. On the contrary, as surveyed in [25, 40, 42], the KDQ can be obtained via a reconstruction protocol that is able to preserve information on the non-commutativity of ρ and the measurement observables. The most relevant properties of KDQ are: (i) $\sum_{\ell,j}q_{\ell,j}(t)=1\ \forall t$; (ii) the *unperturbed* marginals are recovered: $\sum_\ell q_{\ell,j}(t)=p_j(t)=\mathrm{tr}\left\{\rho B_j(t)\right\}$ and $\sum_j q_{\ell,j}(t)=p_\ell(0)=\mathrm{tr}\{\rho A_\ell\}$. The unperturbed marginal at time t cannot be obtained by the TPM scheme if $[\rho,A]\neq0$; (iii) Linearity in the initial state ρ; (iv) KDQ are equal to the joint probabilities

$$p_{\ell,j}^{\mathrm{TPM}}(t)\equiv\mathrm{tr}\left\{A_\ell\rho A_\ell B_j(t)\right\} \tag{2}$$

determined by the TPM scheme when $[\rho,A]=0\ \forall\rho$. In the following, as customary in the literature, we will denote the real part of the KDQ as Margenau–Hill quasiprobability (MHQ) [18, 20, 71, 72].

1.1. Criteria of non-classicality

As mentioned in the introduction, the KDQ may be non-classical. To quantify how far a KDQ is from being a positive real number, any of the following 'quantumness' criteria can be used:

(i) $\mathrm{Re}\left\{q_{\ell,j}(t)\right\} < 0$,
(ii) $\left|\mathrm{Im}\left\{q_{\ell,j}(t)\right\}\right| > s_{\mathrm{th}}$,

where $s_{\mathrm{th}} > 0$ is a threshold value beyond which we can say that the imaginary part is significantly different from zero. This value depends on the specific system under consideration, and we will provide an example in section 4.1. We may similarly define a threshold for the real part without much modification to our results, although we do not follow this approach to keep the notation light. One of our goals in the following is to find how fast the criteria (i) and (ii) can be satisfied[10].

1.2. Real and imaginary parts of KDQ as expectation values of observables

Our strategy is to bound the rate of change of the real and imaginary parts of the KDQ. We can write these two quantities as the expectation values of two different observables. In fact, defining the operators

$$\rho_\ell \equiv \frac{\{\rho, A_\ell\}}{2} \quad \text{and} \quad \sigma_\ell \equiv \frac{[\rho, A_\ell]}{2\mathrm{i}}, \tag{3}$$

which are time-independent and Hermitian, we can write

$$\mathrm{Re}\left\{q_{\ell,j}(t)\right\} = \mathrm{tr}\left\{\rho_\ell B_j(t)\right\} \equiv \langle \rho_\ell \rangle_{j,t}, \tag{4}$$

$$\mathrm{Im}\left\{q_{\ell,j}(t)\right\} = \mathrm{tr}\left\{\sigma_\ell B_j(t)\right\} \equiv \langle \sigma_\ell \rangle_{j,t}. \tag{5}$$

Notice that, if σ_ℓ is the null matrix, then $\mathrm{Im}\left\{q_{\ell,j}(t)\right\} = 0$ for any t and $\mathrm{Re}\left\{q_{\ell,j}(t)\right\}$ reduces to $p^{\mathrm{TPM}}_{\ell,j}(t)$. If $[\rho, A_\ell] \neq 0$ for a given initial density operator ρ, then the KDQ of equation (1) can loose positivity. This occurs if $B_j(t)$ in equation (1) is a projector onto the negative eigenspace of ρ_ℓ [25].

We are going to bound the evolution of quantities of the type

$$\langle X \rangle_{j,t} \equiv \mathrm{tr}\left\{X B_j(t)\right\}. \tag{6}$$

Up to normalization, $B_j(t)$ is in fact a density operator, which justifies the notation of expectation value, albeit it evolves in the Heisenberg representation according to the Hamiltonian $-H$. In the next section, we provide bounds for the evolution of the expectation value of general observables. For the remainder of this article, and for simplicity of notation, we assume that B_j has unit trace. However, the bounds we will derive in the next sections are applicable in the more general case where the trace of B_j is not equal to 1, by re-scaling B_j as $B_j = \mathrm{tr}\left\{B_j\right\}\tilde{B}_j$ where the operator $\tilde{B}_j$ has unit trace. We can then use the linearity of the trace in $\langle X \rangle_{j,t}$ to bring $\mathrm{tr}\left\{B_j\right\}$ outside of the trace and make use of the same bounds.

2. QSL for expectation values of observables

We first derive a result that concerns the time-derivative of the expectation value $\langle X \rangle_t \equiv \mathrm{tr}\{X\rho(t)\}$ with respect to an arbitrary density operator ρ at a given time t.

2.1. Bounding the rate of change using the SR uncertainty relation

Before we present our original contributions, in the next sub-sections, we begin with some well-known results based on the SR uncertainty relation [74]. The SR uncertainty principle for any given observables X, Y and density operator $\rho(t)$ states that

$$\Delta X_t^2 \Delta Y_t^2 \geqslant \left[\left\langle \frac{\{X, Y\}}{2} \right\rangle_t - \langle X \rangle_t \langle Y \rangle_t\right]^2 + \left\langle \frac{[X, Y]}{2\mathrm{i}} \right\rangle_t^2, \tag{7}$$

where $\{\cdot,\cdot\}$ is the anti-commutator, and $\Delta C_t \equiv \sqrt{\langle C^2 \rangle_t - \langle C \rangle_t^2}$ with $C = X, Y$.

[10] A minimal time to non-positivity can be attained even for the quantumness criterion $|\mathrm{Re}\left\{q_{\ell,j}(t)\right\} - p^{\mathrm{TPM}}_{\ell,j}(t)| > k_{\mathrm{th}}$, with k_{th} a given threshold value, as discussed in [73].

The von Neumman equation for the density operator, evolving according to a Hamiltonian H (assumed as time-independent), is written as $\dot{\rho}(t) = [H, \rho(t)]/(\mathrm{i}\hbar) \equiv \{\rho(t), L(t)\}/2$ where L is the symmetric logarithmic derivative. Differentiating $\langle X \rangle_t$ over time leads to

$$\left| \frac{\mathrm{d}}{\mathrm{d}t} \langle X \rangle_t \right| = \left| \left\langle \frac{\{X, L(t)\}}{2} \right\rangle_t \right| \leqslant \Delta L_t \, \Delta X_t, \tag{8}$$

where we used the SR uncertainty relation (7) (see also [74, 75]) and the fact that $\langle L(t) \rangle_t = 0$ for any t, meaning that $\Delta L_t = \sqrt{\langle L^2 \rangle_t}$. By definition, ΔL_t generally represents the square root of the *quantum Fisher information* $\mathcal{F}_Q(t)$ computed with respect to $\rho(t)$: $\Delta L_t = \sqrt{\mathcal{F}_Q(t)}$. It generally holds that $\Delta L_t \leqslant 2\Delta H_t/\hbar \; \forall t$, where the equality applies in the case where ρ is a pure state, whereby we recover the QSL in [28]. Moreover, as shown in appendix A, ΔL is time-independent in our case-study, provided H is constant.

2.2. Explicit bounds on the evolution of $\langle X \rangle_t$

We now present a novel contribution of this work. We derive explicit time-dependent bounds on $\langle X \rangle_t$ by bounding ΔX_t from above, following appendix B. From equation (8), we then arrive at the differential inequality

$$\left| \frac{\mathrm{d}}{\mathrm{d}t} \langle X \rangle_t \right| \leqslant \Delta L \sqrt{(x_1 + x_d) \langle X \rangle_t - \langle X \rangle_t^2 - x_1 x_d}, \tag{9}$$

where $x_1 \leqslant \cdots \leqslant x_d$ are the eigenvalues of X. As a result, integrating (9) results in the bounds (see appendix C)

$$\langle X \rangle_t \geqslant E(X, \tau_0 + \Delta L \, t), \tag{10}$$

$$\langle X \rangle_t \leqslant E(X, \tau_0 - \Delta L \, t), \tag{11}$$

where the function $E(X, \tau)$, which we define below and is illustrated in figure 1, interpolates the maximum and minimum eigenvalues of X:

$$E(X, \tau) \equiv \begin{cases} x_d, & \tau \leqslant 0 \\ x_d \cos^2\left(\frac{\tau}{2}\right) + x_1 \sin^2\left(\frac{\tau}{2}\right), & 0 \leqslant \tau \leqslant \pi \\ x_1, & \tau \geqslant \pi \, . \end{cases} \tag{12}$$

In equations (10) and (11), the initial angle τ_0 is implicitly defined by the equality $E(X, \tau_0) = \langle X \rangle_{t=0}$. We can write it explicitly as $\tau_0 = \tau(X, \langle X \rangle_0)$ with

$$\tau(X, x) \equiv \arccos\left(\frac{2x - x_1 - x_d}{x_1 - x_d} \right). \tag{13}$$

The function $\tau(X, x)$ represents the 'interpolation angle' quantifying where the value x falls between x_1 and x_d (minimal and maximal eigenvalues of X). This notation will be useful in the next section.

2.3. Bounds on derivatives and unified bounds

We can derive a further bound by noting that the derivative $\mathrm{d}\langle X \rangle_t / \mathrm{d}t = \langle \dot{X} \rangle_t$ is itself the expectation value of the observable $\dot{X} \equiv [X, H]/\mathrm{i}\hbar$. Therefore, $\langle \dot{X} \rangle_t$ can be bounded by (10) so that we obtain closed-form bounds as

$$\langle X \rangle_t \geqslant \langle X \rangle_0 + \int_0^{\Delta L t} E\left(\dot{X}, \tau_0' + \xi\right) \mathrm{d}\xi, \tag{14}$$

where τ_0' is implicitly defined by the equality $E(\dot{X}, \tau_0') = \langle \dot{X} \rangle_0$ for $t = 0$. The *unified* lower-bound on $\langle X \rangle_t$ is thus the maximum between the right-hand-sides of equations (10) and (14).

2.4. Saturation of the bounds

Using the Hamiltonian $H = \frac{\hbar\omega}{2} \left(|x_1\rangle\langle x_d| + |x_d\rangle\langle x_1| \right)$, for some real number ω, and $\rho = |x_d\rangle\langle x_d|$ at $t = 0$, the evolution of $\langle X \rangle_t$ exactly matches the right-hand side of the bound (10). The reader can find the technical details in appendix D.

This construction is important as it highlights the geometric interpretation of the inequality (10), whose right-hand side represents the *fastest path*, steered by H, to go from the maximum to the minimum eigenvalue of X.

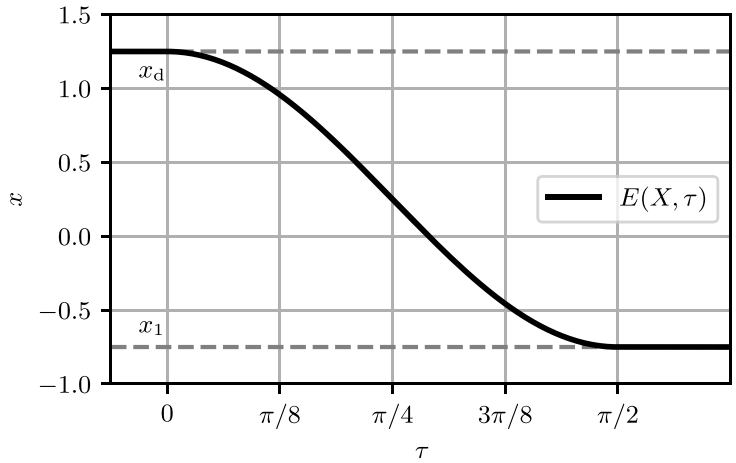

Figure 1. We illustrate the function $E(X,\tau)$, defined in equation (12), that enters the lower and upper bounds (10) and (11). It interpolates the minimum (x_1) and maximum (x_d) eigenvalues of X, using a trigonometric function of the angle τ. The inverse function $\tau(X,x)$, defined in equation (13), returns the angle τ_x such that $E(X,\tau_x)=x$.

3. QSL for Kirkwood–Dirac quasiprobabilities

Following the results of the previous section, we determine time-dependent bounds on the time-derivative of KDQ $q_{\ell,j}(t)$.

The analysis from equations (8) to (14) is valid for a generic Hermitian observable X. We now specialize it to the real and imaginary parts of KDQ by setting $X=\rho_\ell,\sigma_\ell$ in equations (10) and (11) respectively. This leads us to the bounds

$$\mathrm{Re}\left\{q_{\ell,j}(t)\right\} \geqslant E\left(\rho_\ell, \tau^{\mathrm{re}}_{\ell,0}+\Delta L_j t\right), \tag{15}$$

$$\mathrm{Im}\left\{q_{\ell,j}(t)\right\} \geqslant E\left(\sigma_\ell, \tau^{\mathrm{im}}_{\ell,0}+\Delta L_j t\right), \tag{16}$$

where $\tau^{\mathrm{re}}_{\ell,0},\tau^{\mathrm{im}}_{\ell,0}$ are defined by the equality of the bounds at $t=0$, and can be computed using equation (13). Moreover, $L_j(t)$ is the symmetric logarithmic derivative built on the Hamiltonian $-H$ and the state $B_j(t)$ such that $\mathrm{d}B_j(t)/\mathrm{d}t=[-H,B_j(t)]/\mathrm{i}\hbar=\{B_j(t),L_j(t)\}/2$. Thus, the standard deviation $\Delta L_{j,t}$ is also computed with respect to $B_j(t)$, i.e. $\Delta L_{j,t}=\sqrt{\langle L_j(t)^2\rangle_t}=\mathrm{tr}\{L_j(t)^2B_j(t)\}$. It is worth noting that, following the same steps in appendix A, we can prove that ΔL_j is time-independent for all j, provided H is constant.

Finally, replacing $\dot{X}=\dot{\rho}_\ell,\dot{\sigma}_\ell$ in equation (14) can lead to more refined bounds on the real and imaginary parts of the KDQ, as also shown in figure 2 for the internal energy variations of a qubit subject to a controlled-unitary gate.

3.1. Commutative limit

Let us focus on the case of $[\rho,A_\ell]=0$, whereby the KDQ are equal to the joint probabilities returned by the TPM scheme (equation (2)) that, by definition, are always positive and $\in[0,1]$. If $[\rho,A_\ell]=0$, then the imaginary part of the KDQ is zero. Given $A_\ell\neq\mathbb{I}$ with $\mathbb{I}$ the identity operator, the minimum eigenvalue of ρ_ℓ (here equal to $A_\ell\rho A_\ell$) is $r_1=0$. As a result, from equation (15), one has that

$$p^{\mathrm{TPM}}_{\ell,j}(t) \geqslant r_d\cos^2\left(\frac{\tau^{\mathrm{re}}_{\ell,0}+\Delta L_j t}{2}\right). \tag{17}$$

Hence, as expected, no negativity can be observed from equation (17).

3.2. Time to non-positivity

The bounds equations (15) and (16) allow us to derive minimal times to non-positivity. Following the two criteria (i) and (ii) of non-classicality in section 1.1, we ask how long it takes for the right-hand sides of (15) and (16) to go from their initial values to the target values of 0 and s_{th} respectively, namely what are the times $T^{\mathrm{re}}_{\ell,j},T^{\mathrm{im}}_{\ell,j}$ such that $E(\rho_\ell,\tau^{\mathrm{re}}_{\ell,0}+\Delta L_j T^{\mathrm{re}}_{\ell,j})=0$ and $E(\sigma_\ell,\tau^{\mathrm{im}}_{\ell,0}+\Delta L_j T^{\mathrm{im}}_{\ell,j})=s_{\mathrm{th}}$. Using equation (13), the initial and target values can be expressed in terms of the function $\tau(X,x)$. As a result, for the (ℓ,j)th KDQ, the minimal times $T^{\mathrm{re}}_{\ell,j},T^{\mathrm{im}}_{\ell,j}$ read respectively as

$$T^{\mathrm{re}}_{\ell,j}=\frac{\tau\left(\rho_\ell,0\right)-\tau^{\mathrm{re}}_{\ell,0}}{\Delta L_j}, \tag{18}$$

$$T^{\rm im}_{\ell,j} = \frac{\tau\left(\sigma_\ell, s_{\rm th}\right) - \tau^{\rm im}_{\ell,0}}{\Delta L_j}\,. \tag{19}$$

Equation (18) coincides with the Mandelstam's and Tamm's result [30, 31] in the following circumstance: $\rho = |\psi\rangle\langle\psi|$ is a pure state, A_ℓ is the identity (i.e. no measurement is performed at time $t = 0$), and $B_j(t) = \rho$ at a given time t. Under these assumptions, indeed, $T^{\rm re}_{\ell j} = \hbar\pi\,/\,(2\Delta H)$. Hence, in analogy, we can still interpret $T^{\rm re}_{\ell j}$ as the minimum time for a quantum system to evolve towards an orthogonal state, even in the more general setting with non-commutative observables and initial state.

4. Enhancing power extraction

Non-commutativity between the initial state ρ and a time-dependent Hamiltonian implementing a work protocol can be a resource to *enhance quantum work extraction* beyond what can be achieved by any classical system [20, 42, 76]. To this end, let us recall the definition of the extractable work $W_{\rm ext}(t)$ at time t in a coherently-driven closed quantum system. We make use of the spectral decomposition of the system Hamiltonian, $H(t_k) = \sum_n E_n(t_k)\Pi_n(t_k)$, with $k = 1, 2$, $n \in \{\ell, j\}$ and $\{\Pi_n(t_k)\}$ denoting the sets of projectors over the energy basis. $W_{\rm ext}(t)$ is thus defined as [77, 78]

$$\begin{aligned} W_{\rm ext}\left(t\right) \equiv -\langle w(t)\rangle = \sum_{\ell,j}\left(E_\ell\left(0\right) - E_j\left(t\right)\right) q_{\ell,j}\left(t\right) = \\ = {\rm tr}\{\rho H(0)\} - {\rm tr}\left\{U\rho U^\dagger H(t)\right\}, \end{aligned} \tag{20}$$

where $w(t) \equiv E(t) - E(0)$ is the *stochastic work* so that $w_{\ell,j}(t) \equiv E_j(t) - E_\ell(0)$. A necessary condition to enhance $W_{\rm ext}(t)$, beyond the maximum value achievable classically, is that ${\rm Re}\left\{q_{\ell,j}(t)\right\} < 0$ for some time t [20]. Negative MHQ allow for *anomalous energy transitions*, i.e. work realizations $w_{\ell,j}$ that occur with a negative quasiprobability. Thus, if negative MHQ are associated with positive $w_{\ell,j}$, then the extractable work is boosted.

Considering time constraints is important in quantum engines and energy conversion devices [79–82], where the energy power depends on the times in which the strokes of a given machine are accurately performed. Thus, for work extraction purposes, one would like to achieve the maximum possible value of $W_{\rm ext}(t)$ in the shortest possible time. This means that, if also a boost of work extraction due to negative MHQ is included, then one needs to derive the minimum time at which ${\rm Re}\left\{q_{\ell,j}(t)\right\} < 0$ for positive work realizations $w_{\ell,j}(t) > 0$. At the same time, the MHQ associated with negative $w_{\ell,j}(t)$ have to be positive. Hence, the optimization of the work extraction in finite-time transformations requires to maximize the *work extraction power*, which is defined by $\mathcal{P}(t) \equiv -\langle w(t)\rangle / T_{\rm max}$, where $T_{\rm max}$ is the time for maximum extractable work [76].

The optimal value of $\mathcal{P}$ comes from a trade-off between maximum extractable work (even enhanced by negativity) and minimum time period $T_{\rm max}$. Such an optimal $\mathcal{P}$ could be bounded by an approximated power function computed using the minimal time $T^{\rm re}_{\ell j}$ to negative quasiprobabilities.

4.1. Two-qubit example

We conclude the analysis by verifying our bounds on both the real and imaginary parts of KDQ, as well as the bound on $\mathcal{P}$ using $T^{\rm re}_{\ell j}$ for the two-qubit controlled-unitary gate experimentally realized in [60]. The gate evolves according to the time-independent Hamiltonian

$$H_{\rm 2qubits} = \frac{\omega_L}{2}\left(Z_1 + Z_2\right) + \frac{\omega_{\rm int}}{2}|1\rangle\langle 1| \otimes X, \tag{21}$$

where Z_i is the Z-Pauli matrix applied to the qubit i, X is the X-Pauli matrix, and $|0\rangle, |1\rangle$ are respectively the ground and excited states of the local Hamiltonian of each qubit. The first qubit acts as a 'control' knob: if it is in the excited state, the second qubit ('target') undergoes a rotation of a parameterized angle.

In this process, the internal energy of the target qubit changes with time, as provided by computing the partial trace of the two-qubit state with respect to the degrees of freedom of the control qubit. Assuming the control qubit can be manipulated at will, we interpret the internal energy variation of the target qubit as thermodynamic work exerted by the control qubit. We compute the KDQ of the internal energy variation of the target qubit by setting $A_\ell = |\ell\rangle\langle\ell|$ and $B_j = |j\rangle\langle j|$ with $\ell, j = 0, 1$. Preparing the global system in the state $|-\rangle|1\rangle$, where $|-\rangle \equiv (|0\rangle - |1\rangle)/\sqrt{2}$, leads to non-positivity of the computed KDQ. Here, negativity is a signature of extractable work from the target qubit, in a regime where the corresponding value returned by the TPM scheme, $W^{\rm TPM}_{\rm ext}(t) \equiv \sum_{\ell,j}(E_\ell(0) - E_j(t))p^{\rm TPM}_{\ell,j}(t)$, is zero for any parameters choice, due to the state-collapse upon the first energy measurement of the TPM scheme and the specific choice of the initial state for the global system.

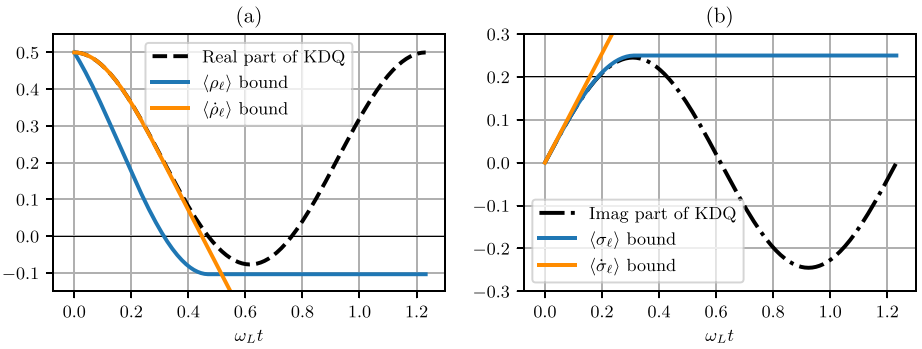

Figure 2. Quasiprobability associated to the internal energy variations of the target qubit in a two-qubit controlled-unitary gate with Hamiltonian $H_{2\text{qubits}}$. *Black line*: Real [panel (a)] and imaginary [panel (b)] parts of the KDQ $q_{1,1}(t)$ using $A_1 = B_1 = |1\rangle\langle 1|$, with $\{|0\rangle, |1\rangle\}$ computational basis. Globally the quantum gate is initialized in the pure state $|-\rangle\,|1\rangle$. Negativity in $\mathrm{Re}\{q_{1,1}(t)\}$ is observed choosing $\omega_L = 1$ and $\omega_{\text{int}} = 5$. *Blue and orange lines*: Lower-bounds to the quasiprobability, both derived from the uncertainty principle (7). They are respectively obtained by constraining the evolution of $\langle\rho_1\rangle_{1,t}, \langle\sigma_1\rangle_{1,t}$ (equations (15) and (16)) (blue lines), and $\langle\dot{\rho}_1\rangle_{1,t}, \langle\dot{\sigma}_1\rangle_{1,t}$ (equation (14) with $X = \dot{\rho}_\ell, \dot{\sigma}_\ell$) (orange lines).

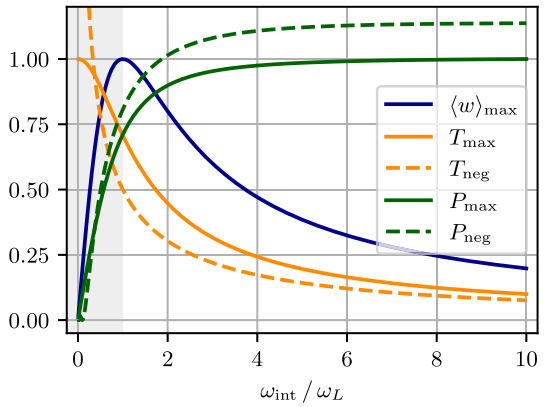

Figure 3. The time to negativity T_{neg} (dashed orange) acts as a lower-bound to the time $T_{\max}$ (solid orange), at which the maximum average work $\langle w\rangle_{\max}$ (blue) is extracted from the target qubit under conditions of figure 2. The power at maximum energy extraction, $\mathcal{P}_{\max} = \langle w\rangle_{\max}/T_{\max}$ (solid green), can be well-approximated by the power $\mathcal{P}_{\text{neg}}$ computed at T_{neg} (dashed green). $\mathcal{P}_{\text{neg}}$ is an upper-bound of $\mathcal{P}_{\max}$. This reasoning cannot be applied to the light gray region, since the negativity is not present. The value of the energies, times and powers are respectively normalized by $E_{\text{ref}} = 0.5$, $t_{\text{ref}} = \pi$ and $\mathcal{P}_{\text{ref}} \approx 0.32$.

In figures 2(a) and (b) we plot the real and imaginary parts of the quasiprobability $q_{1,1}(t)$ (i.e. $\ell, j = 1$), respectively, together with the lower-bounds (14) with $\dot{X} = \dot{\rho}_\ell, \dot{\sigma}_\ell$, and (15), (16), for $\omega_L = 1$ and $\omega_{\text{int}} = 5$. One has to take the tightest between the blue and orange curves as the lower-bound to $\mathrm{Re}\{q_{1,1}(t)\}$, $\mathrm{Im}\{q_{1,1}(t)\}$ for any time t. In figure 2(a), the first time to negativity (given by crossing the threshold at $\mathrm{Re}\{q_{1,1}\} = 0$) is well identified by the lower-bound (14), while the first time $\mathrm{Im}\{q_{1,1}(t)\}$ touches the threshold set at 0.2 is provided by the lower-bound (16). This choice to set the threshold of $\mathrm{Im}\{q_{1,1}\}$ at 0.2 is dictated by the evidence that, in possible experiments as recently in [55], the error bars in reconstructing the imaginary part of a quasiprobability are around 10% of the actual value.

In figure 3, we plot the time to negativity T_{neg}, which is defined as the time at which the bound of $\langle\dot{\rho}_\ell\rangle_{j,t}$ (equation (14) with $X = \dot{\rho}_\ell$) in figure 2 reaches zero. T_{neg} is a lower-bound of the time $T_{\max}$ at which the maximum amount of energy can be possibly extracted from the target qubit. The work extraction power $\mathcal{P}_{\text{neg}}$ obtained at T_{neg} turns out to be a good approximation for the power $\mathcal{P}_{\max}$ at $T_{\max}$. Notably, it is an upper-bound that can be experimentally measured via local measurements.

5. Conclusions

We have derived time-dependent bounds for the Kirkwood–Dirac quasiprobabilities, which stem from using the SR uncertainty relation on the time-derivative of such quasiprobabilities. Our derivation can be interpreted as an extension to non-commutative operators of the QSL bound obtained by Mandelstam and Tamm.

The first consequence of our results is to determine the minimal time it takes for the real part of a KDQ to become negative, and for the corresponding imaginary part to go from zero to exceed a threshold value. The minimal time to negativity has an application as a bound on the maximum power of a finite-time work extraction process. Consequently, we suggest to further investigate more complex quantum gates [83], and devices for energy conversion [79–81] including quantum batteries [82]. Moreover, the QSL time-bound on KDQ could also predict abrupt or anomalous changes in out-of-time-ordered correlators, which can be equivalently expressed as the characteristic function of a KDQ distribution [9, 34, 42].

Data availability statement

There was no data generated for this article. The data that support the findings of this study are available upon reasonable request from the authors.

Acknowledgments

S S P acknowledges support from the 'la Caixa' foundation through scholarship No. LCF/BQ/DR20/1179 0030, and from national funds by FCT—Fundação para a Ciência e Tecnologia, I.P., through scholarship 2023.01162.BD, and in the framework of the Projects UIDB/04564/2020 and UIDP/04564/2020, with DOI identifiers https://doi.org/10.54499/UIDB/04564/2020 and https://doi.org/10.54499/UIDP/04564/2020, respectively. S G acknowledges financial support from the Project PRIN 2022 Quantum Reservoir Computing (QuReCo), the PNRR MUR Project PE0000023-NQSTI financed by the European Union–Next Generation EU, and the MISTI Global Seed Funds MIT-FVG Collaboration Grant 'Revealing and exploiting quantumness via quasiprobabilities: from quantum thermodynamics to quantum sensing'. S D acknowledges support from the U.S. National Science Foundation under Grant No. DMR-2010127 and the John Templeton Foundation under Grant No. 62422.

Appendix A. Proof I: bounds on the expectation value using the Hamiltonian and symmetric logarithmic derivative

In the main text, $B_j(t)$ plays the role of a (unnormalized) density operator ρ. In this section, we derive bounds on the evolution-rate for the expectation value of an observable X, taken with respect to ρ. Suppose ρ evolves unitarily as $\rho(t) = U\rho(0)U^\dagger$, with $U = \exp(-\mathrm{i}Ht/\hbar)$ for some constant Hermitian operator H, so that

$$\frac{\mathrm{d}\rho(t)}{\mathrm{d}t} = \frac{[H,\rho(t)]}{\mathrm{i}\hbar}. \tag{A.1}$$

Another way to write the evolution of ρ is using the symmetric logarithmic derivative operator L that is defined implicitly, for all times, by

$$\frac{\mathrm{d}\rho(t)}{\mathrm{d}t} \equiv \frac{1}{2}\{\rho(t), L(t)\}. \tag{A.2}$$

The spectral decomposition $\rho = \sum_j p_j |j\rangle\langle j|$ allows us to write L in the basis $\{|j\rangle\}$, such that

$$L_{ij} = \frac{2}{\mathrm{i}\hbar}\frac{p_j - p_i}{p_i + p_j}H_{ij}, \tag{A.3}$$

where $L_{ij} \equiv \langle i|L|j\rangle$ and $H_{ij} \equiv \langle i|H|j\rangle$. If $p_i = p_j = 0$, then we take L_{ij} equal to zero. Moreover, for a constant Hamiltonian H, we can take

$$L(t) = UL(0)U^\dagger, \tag{A.4}$$

which is compatible with the definition of L for any time t, that is,

$$\frac{\{\rho(t), L(t)\}}{2} = U\frac{\{\rho(0), L(0)\}}{2}U^\dagger = U\frac{[H,\rho(0)]}{\mathrm{i}\hbar}U^\dagger = \frac{[H,\rho(t)]}{\mathrm{i}\hbar} = \dot{\rho}(t). \tag{A.5}$$

As a result, we have two ways to bound the evolution of the expectation value $\langle X\rangle_t$. The first way follows the Hamiltonian formalism:

$$\left|\frac{\mathrm{d}\langle X\rangle_t}{\mathrm{d}t}\right| = \left|\left\langle\frac{[X,H]}{\mathrm{i}\hbar}\right\rangle_t\right| \leqslant \frac{2}{\hbar}\Delta H\Delta X_t, \tag{A.6}$$

where we used the SR uncertainty relation (7) with $Y = H$.

The second bound, making use of the symmetric logarithmic derivative, reads as

$$\left|\frac{\mathrm{d}\langle X\rangle_t}{\mathrm{d}t}\right| = \left|\left\langle \frac{\{X,L\}}{2}\right\rangle_t\right| \leqslant \Delta L_t \Delta X_t, \tag{A.7}$$

where we used the replacement $Y = L(t)$. Note that, using the definition of L, we have $\langle L(t)\rangle_t = 0\ \forall t$.

We note that, if H is constant, then also ΔL is constant. Indeed, using that $L(t) = UL(0)U^\dagger$ like $\rho(t) = U\rho(0)U^\dagger$, we get:

$$\Delta L_t^2 = \left\langle L(t)^2\right\rangle_t = \mathrm{tr}\left\{\rho(t)\,L(t)^2\right\} = \mathrm{tr}\left\{\rho(0)\,L(0)^2\right\} = \Delta L^2 \quad \forall t, \tag{A.8}$$

which implies that ΔL_t^2 is constant. This fact allows to calculate the bounds at $t = 0$ without solving for the system dynamics.

It turns out that, if $\mathrm{rank}(\rho) = 1$, then the two bounds (A.6) and (A.7) are equal. This can be shown by setting $\rho = |\varphi\rangle\langle\varphi|$, whereby

$$\frac{\Delta L^2}{2} = \mathrm{tr}\left\{\left(\frac{\{\rho(t), L(t)\}}{2}\right)^2\right\} = \mathrm{tr}\left\{\left(\frac{[H,\rho(t)]}{\mathrm{i}\hbar}\right)^2\right\} = \frac{2\Delta H^2}{\hbar^2}, \tag{A.9}$$

i.e. $\Delta L = 2\,\Delta H/\hbar$, meaning that the two bounds (A.6) and (A.7) coincide.

More in general instead ($\mathrm{rank}(\rho) > 1$), the use of ΔL results in a tighter bound. To see this, let us equate the right-hand sides of (A.1) and (A.2), multiply them by $L(t)$, and take the trace. This results in

$$\Delta L^2 = \left\langle \frac{[L(t), H]}{\mathrm{i}\hbar}\right\rangle_t \leqslant \frac{2}{\hbar}\Delta L\,\Delta H, \tag{A.10}$$

where the inequality comes from the uncertainty principle. Therefore, in general,

$$\Delta L \leqslant \frac{2}{\hbar}\,\Delta H \tag{A.11}$$

that proves that using the symmetric logarithmic derivative provides a tighter bound.

Appendix B. Proof II: upper bound on the variance of a Hermitian operator

When calculating the bounds on quasiprobabilities using the SR uncertainty relation, we are led to a differential equation depending on $\Delta X \equiv \sqrt{\langle X^2\rangle - \langle X\rangle^2}$ with X being a generic Hermitian operator. The quantity ΔX can be bounded using only the expectation value $\langle X\rangle = \mathrm{tr}\{X\rho\}$, namely

$$\begin{aligned}\Delta X^2 &= \left\langle X^2\right\rangle - \langle X\rangle^2 \\ &\leqslant (x_1 + x_d)\,\langle X\rangle - x_1 x_d - \langle X\rangle^2,\end{aligned} \tag{B.1}$$

where x_1, x_d are respectively the lowest and highest eigenvalues of X.

To derive equation (B.1), we use the following proposition.

Proposition 1. *Let X be a Hermitian operator with eigenvalues $x_1 \leqslant \cdots \leqslant x_d$ and ρ a density operator. Then,*

$$\langle X^2\rangle \leqslant (x_1 + x_d)\,\langle X\rangle - x_1 x_d. \tag{B.2}$$

Proof. Notice that $x_1\mathbb{I} \preceq X \preceq x_d\mathbb{I}$, where $\mathbb{I}$ is the identity operator. Hence, $(X - x_1\mathbb{I})$ and $(x_d\mathbb{I} - X)$ are both positive semidefinite operators, such that by multiplying them one has

$$(X - x_1\mathbb{I})\,(x_d\mathbb{I} - X) \succeq 0. \tag{B.3}$$

Expanding and rearranging (B.3), we get

$$X^2 \preceq (x_1 + x_d)\,X - x_1 x_d\mathbb{I}. \tag{B.4}$$

Therefore, taking the expectation value with respect to ρ, we arrive at the desired result. □

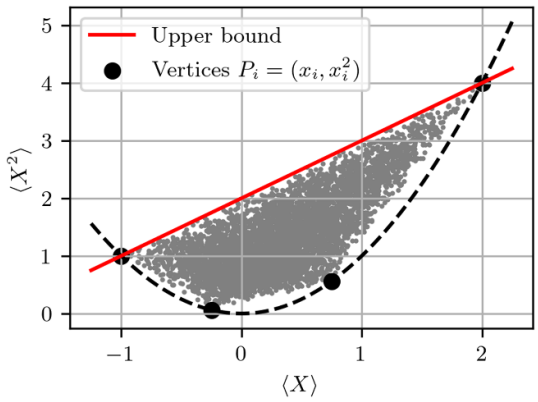

Figure B1. Illustration of inequality (B.2). For a Hermitian operator X with eigenvalues $x_1 \leqslant \cdots \leqslant x_d$, the set of possible points $(\langle X \rangle, \langle X^2 \rangle)$ (gray dots) forms a convex polygon, whose vertices $P_i = (x_i, x_i^2)$ lie on a common parabolic path (dashed line). Since a parabola is a convex function, any $\langle X^2 \rangle$ can be bounded from above using the secant joining the vertices P_1 and P_d (red line).

To conclude, in figure B1 we illustrate the inequality (B.2) and how it works.

Appendix C. Proof III: solution of the differential inequality of equation (9)

In this appendix we solve the following differential inequality of equation (9) that we express in a more compact form as

$$\left|\frac{\mathrm{d}x}{\mathrm{d}t}\right| \leqslant \omega\sqrt{(a+b)x - x^2 - ab}, \tag{C.1}$$

where $x = x(t)$ is a time-dependent variable, and $\omega \geqslant 0$ and $a \leqslant b$ are two real constants. Also notice that the function x is bounded as $a \leqslant x(t) \leqslant b$ for all times t. By defining $x \equiv \alpha z + \beta$, with $\alpha \equiv (b-a)/2$ and $\beta \equiv (a+b)/2$ (i.e. $a = \beta - \alpha$ and $b = \alpha + \beta$), we get the reduced form

$$\left|\frac{\mathrm{d}z}{\mathrm{d}t}\right| \leqslant \omega\sqrt{1 - z^2}\,. \tag{C.2}$$

Let us focus on the negative branch of the differential inequality (C.2), since the positive branch has an analogous solution. The negative branch of (C.2) can be solved by substituting

$$z = \cos(\tau) \quad \Longleftrightarrow \quad \mathrm{d}z = -\sin(\tau)\,\mathrm{d}\tau\,. \tag{C.3}$$

This is because the lower bound of (C.2) entails the separable differential inequality

$$\frac{\mathrm{d}z}{\sqrt{1-z^2}} \geqslant -\omega\,\mathrm{d}t. \tag{C.4}$$

Upon the substitution (C.3), this simplifies to

$$\frac{\mathrm{d}\tau}{\mathrm{d}t} \leqslant \omega \quad \Longrightarrow \quad \tau(t) \leqslant \tau_0 + \omega t, \tag{C.5}$$

where τ_0 is the value of τ at the initial time ($t = 0$, in the main text of the paper) of the interval in which the differential inequality (C.1) is solved. In this way, by replacing back z and x, and using the fact that the cosine is decreasing in the region $[0, \pi]$, we get

$$x(t) \geqslant \begin{cases} \alpha\cos(\tau_0 + \omega t) + \beta, & \text{for } t < t^* \\ a, & \text{for } t \geqslant t^* \end{cases} \tag{C.6}$$

where $\tau_0 = \arccos((x(0) - \beta)/\alpha) \in [0, \pi]$ and $t^* = (\pi - \tau_0)/\omega$. The solution is divided into branches because, despite the oscillating solution, the lower bound of $x(t)$ can never increase in value, given that the lower branch of the inequality (C.1) (symmetric with respect to 0) is never positive. For the sake of clarity, see figure C1 for a visual representation of the solution (C.6), concerning the real part of an actual

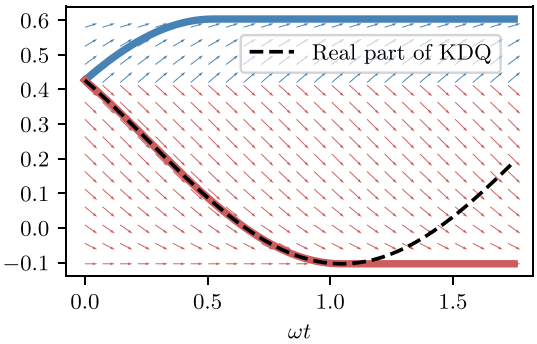

Figure C1. Upper and lower bounds (blue and red lines respectively) of the real part of the Kirkwood–Dirac quasiprobability $q_{1,1}(t)$ as a function of time (in dimensionless units). The bounds are obtained by integrating the differential inequality (C.1). It can be observed that the lower bound is saturated, being superimposed on the quasiprobability. The blue arrows represent the gradient field of the upper bound, while the red arrows correspond to the gradient field of the lower bound. The black dotted line depicts the time-evolution of $q_{1,1}(t)$. The quasiprobability drawn in the figure comes from taking $(|0\rangle + |1\rangle)/\sqrt{2}$ as the initial state, and $A_1 = |0\rangle\langle 0|$ as the projector of the initial measurement at $t = 0$. The quantum system evolves unitarily under the Hamiltonian $H = \frac{\hbar\omega}{2}(|r_1\rangle\langle r_d| + |r_d\rangle\langle r_1|)$, where $|r_1\rangle, |r_d\rangle$ are the eigenvectors of $\rho_1 \equiv \{\rho, A_1\}/2$ associated to the minimum and maximum eigenvalues r_1 and r_d, respectively. The projector of the second measurement (at time t) is $B_1 = |\psi\rangle\langle\psi|$, where $|\psi\rangle = \cos(\frac{\pi}{6})|r_1\rangle - i\sin(\frac{\pi}{6})|r_d\rangle$.

Kirkwood–Dirac quasiprobability (KDQ). Therefore, there is a time interval (from 0 to t^*) for the analytical solution to be valid; beyond $t = t^*$, the lower bound must remain constant and equal to a.

Using standard trigonometric identities, we may rewrite the bound as

$$x(t) \geqslant F(\tau_0 + \omega t), \tag{C.7}$$

where

$$F(\tau) \equiv \begin{cases} b\cos^2\left(\frac{\tau}{2}\right) + a\sin^2\left(\frac{\tau}{2}\right) & 0 \leqslant \tau \leqslant \pi \\ a & \tau \geqslant \pi \end{cases}. \tag{C.8}$$

The positive branch of the differential equation (C.2) can be integrated similarly to the negative branch, with the result that

$$x(t) \leqslant F'(\tau_0 - \omega t), \tag{C.9}$$

where F' is similarly defined as

$$F'(\tau) \equiv \begin{cases} b\cos^2\left(\frac{\tau}{2}\right) + a\sin^2\left(\frac{\tau}{2}\right) & 0 \leqslant \tau \leqslant \pi \\ b & \tau \leqslant 0. \end{cases} \tag{C.10}$$

Since we assumed only $t \geqslant 0$, the domain of the functions F and F' overlap only in the interval $[0, \pi]$ where they coincide. Therefore, we can write the bounds using a unified function E,

$$E(\tau) \equiv \begin{cases} b & \tau \leqslant 0 \\ b\cos^2\left(\frac{\tau}{2}\right) + a\sin^2\left(\frac{\tau}{2}\right) & 0 \leqslant \tau \leqslant \pi \\ a & \tau \geqslant \pi, \end{cases} \tag{C.11}$$

and thus obtain

$$x(t) \geqslant E(\tau_0 + \omega t), \tag{C.12}$$

$$x(t) \leqslant E(\tau_0 - \omega t), \tag{C.13}$$

for $t \geqslant 0$.

Appendix D. Proof IV: saturation of the bounds

The bounds (C.12) and (C.13) can be saturated. In figure C1, we show an example where the real part of a KDQ is saturated. Let us now explain under which conditions the saturation of the bounds is achieved.

Let X be an observable with eigenvalues $x_1 \leqslant \cdots \leqslant x_d$, corresponding to the eigenvectors $|x_1\rangle, \ldots, |x_d\rangle$, respectively. Then, let us consider an initial state $\rho = |\psi\rangle\langle\psi|$ in the subspace generated by $|x_1\rangle, |x_d\rangle$, for example

$$|\psi\rangle = \cos\left(\frac{\tau_0}{2}\right)|x_d\rangle - \mathrm{i}\sin\left(\frac{\tau_0}{2}\right)|x_1\rangle, \tag{D.1}$$

for some angle τ_0 in $[0, 2\pi]$. Suppose also that the system evolves according to the Hamiltonian

$$H = \frac{\hbar\omega}{2}\left(|x_1\rangle\langle x_d| + |x_d\rangle\langle x_1|\right), \tag{D.2}$$

so that the system never leaves the subspace spanned by $\{|x_1\rangle\langle x_1|, |x_d\rangle\langle x_d|\}$. In this subspace, the unitary operator can be represented as

$$U \to \begin{pmatrix} \cos(\omega t/2) & -\mathrm{i}\sin(\omega t/2) \\ -\mathrm{i}\sin(\omega t/2) & \cos(\omega t/2) \end{pmatrix} \tag{D.3}$$

that leads to

$$\langle X\rangle_t = x_d \cos^2\left(\frac{\tau_0 + \omega t}{2}\right) + x_1 \sin^2\left(\frac{\tau_0 + \omega t}{2}\right). \tag{D.4}$$

Equation (D.4) matches either the bound (C.12) or (C.13) depending on the value of τ_0. If $\tau_0 \in [0, \pi]$, then the expectation value in equation (D.4) coincides with the time-varying branch of the lower bound (C.12). On the other hand, if $\tau_0 \in [\pi, 2\pi]$, then $\cos^2((\tau_0 + \omega t)/2) = \cos^2((\tau_0 - \omega t)/2)$ such that equation (D.4) saturates the upper bound (C.13). Notice that this reasoning is true because we have assumed that ρ is a pure state, which means: $\Delta L = 2\Delta H/\hbar = \omega$.

The saturation of the bounds for $\langle X\rangle_t$ entails also the saturation of the bounds on the evolution of the real and imaginary parts of KDQ. In fact, let us consider, for example, the real part of the KDQ $q_{1,1}(t)$ in figure C1. In this case, the observable X is the operator $\rho_1 = \{\rho, A_1\}/2$, where ρ is the density operator associated to the pure quantum state, and A_1 is a rank-1 projector. We denote with $r_1 \leqslant \ldots \leqslant r_d$ the eigenvalues of ρ_1, and with $|r_1\rangle, \ldots, |r_d\rangle$ the corresponding eigenvectors, respectively. All the other eigenvalues besides r_1 and r_d are zero, in this case. Then, we consider the Hamiltonian $H = -\frac{\hbar\omega}{2}\left(|r_1\rangle\langle r_d| + |r_d\rangle\langle r_1|\right)$, and the operator $B_1 = |\psi\rangle\langle\psi|$ that plays the role of the operator ρ with respect to which $\langle X\rangle_t$ is computed. In B_1, $|\psi\rangle = \cos(\frac{\tau_0}{2})|r_1\rangle - \mathrm{i}\sin(\frac{\tau_0}{2})|r_d\rangle$ for some angle $\tau_0 \in [0, 2\pi]$. Using the same reasoning of the previous paragraph, we can determine that

$$\mathrm{Re}\{q_{1,1}(t)\} = \mathrm{tr}\{\rho_1 U^\dagger B_1 U\} \equiv \langle\rho_1\rangle_{1,t} \tag{D.5}$$

saturates one of the bounds among (C.12) and (C.13) for a specific value of τ_0, as illustrated in figure C1.

ORCID iDs

Sagar Silva Pratapsi https://orcid.org/0000-0002-1633-4414
Sebastian Deffner https://orcid.org/0000-0003-0504-6932
Stefano Gherardini https://orcid.org/0000-0002-9254-507X

References

[1] Nielsen M A and Chuang I L 2010 *Quantum Computation and Quantum Information* (Cambridge University Press)
[2] Leggett A J and Garg A 1985 Quantum mechanics versus macroscopic realism: is the flux there when nobody looks? *Phys. Rev. Lett.* **54** 857–60
[3] Ollivier H and Zurek W H 2001 Quantum discord: a measure of the quantumness of correlations *Phys. Rev. Lett.* **88** 017901
[4] Margenau H and Hill R N 1961 Correlation between measurements in quantum theory *Prog. Theor. Phys.* **26** 722–38
[5] Silva A 2008 Statistics of the work done on a quantum critical system by quenching a control parameter *Phys. Rev. Lett.* **101** 120603
[6] Chenu A, Egusquiza I L, Molina-Vilaplana J and Campo A 2018 Quantum work statistics, Loschmidt echo and information scrambling *Sci. Rep.* **8** 1–8
[7] Dressel J, González Alonso J R, Waegell M and Yunger Halpern N 2018 Strengthening weak measurements of qubit out-of-time-order correlators *Phys. Rev. A* **98** 012132

[8] González Alonso J R, Yunger Halpern N and Dressel J 2019 Out-of-time-ordered-correlator quasiprobabilities robustly witness scrambling *Phys. Rev. Lett.* **122** 040404
[9] Mohseninia R, González Alonso J R and Dressel J 2019 Optimizing measurement strengths for qubit quasiprobabilities behind out-of-time-ordered correlators *Phys. Rev. A* **100** 062336
[10] Touil A and Deffner S 2020 Quantum scrambling and the growth of mutual information *Quantum Sci. Technol.* **5** 035005
[11] Touil A and Deffner S 2021 Information scrambling versus decoherence—two competing sinks for entropy *PRX Quantum* **2** 010306
[12] Tripathy D, Touil A, Gardas B and Deffner S 2024 Quantum information scrambling in two-dimensional Bose-Hubbard lattices *Chaos* **34** 043121
[13] Carolan E, Kiely A, Campbell S and Deffner S 2024 Operator growth and spread complexity in open quantum systems *Europhys. Lett.* **147** 38002
[14] Talkner P, Lutz E and Hänggi P 2007 Fluctuation theorems: work is not an observable *Phys. Rev. E* **75** 050102(R)
[15] Kafri D and Deffner S 2012 Holevo's bound from a general quantum fluctuation theorem *Phys. Rev. A* **86** 044302
[16] Solinas P and Gasparinetti S 2016 Probing quantum interference effects in the work distribution *Phys. Rev. A* **94** 052103
[17] Díaz M G, Guarnieri G and Paternostro M 2020 Quantum work statistics with initial coherence *Entropy* **22** 1223
[18] Levy A and Lostaglio M 2020 Quasiprobability distribution for heat fluctuations in the quantum regime *PRX Quantum* **1** 010309
[19] Maffei M, Elouard C, Goes B O, Huard B, Jordan A N and Auffèves A 2023 Anomalous energy exchanges and Wigner-function negativities in a single-qubit gate *Phys. Rev. A* **107** 023710
[20] Hernández-Gómez S, Gherardini S, Belenchia A, Lostaglio M, Levy A and Fabbri N 2024 Projective measurements can probe nonclassical work extraction and time correlations *Phys. Rev. Res.* **6** 023280
[21] Francica G and Dell'Anna L 2023 Quasiprobability distribution of work in the quantum Ising model *Phys. Rev. E* **108** 014106
[22] Touil A and Deffner S 2024 Information scrambling—a quantum thermodynamic perspective *Europhys. Lett.* **146** 48001
[23] Buscemi F, Dall'Arno M, Ozawa M and Vedral V 2014 Universal optimal quantum correlator *Int. J. Quantum Inf.* **12** 1560002
[24] Solinas P, Amico M and Zanghì N 2021 Measurement of work and heat in the classical and quantum regimes *Phys. Rev. A* **103** L060202
[25] Lostaglio M, Belenchia A, Levy A, Hernández-Gómez S, Fabbri N and Gherardini S 2023 Kirkwood–Dirac quasiprobability approach to the statistics of incompatible observables *Quantum* **7** 1128
[26] Pandey V, Shrimali D, Mohan B, Das S and Pati A K 2023 Speed limits on correlations in bipartite quantum systems *Phys. Rev. A* **107** 052419
[27] Deffner S and Campbell S 2017 Quantum speed limits: from Heisenberg's uncertainty principle to optimal quantum control *J. Phys. A: Math. Theor.* **50** 453001
[28] Mohan B and Pati A K 2022 Quantum speed limits for observables *Phys. Rev. A* **106** 042436
[29] Carabba N, Hörnedal N and Campo A 2022 Quantum speed limits on operator flows and correlation functions *Quantum* **6** 884
[30] Mandelstam L I and Tamm I E 1945 The uncertainty relation between energy and time in nonrelativistic quantum mechanics *J. Phys.* **9** 249–54
[31] Mandelstam L and Tamm I G 1991 The uncertainty relation between energy and time in non-relativistic quantum mechanics *Selected Papers* (Springer) pp 115–23
[32] Robertson H P 1929 The uncertainty principle *Phys. Rev.* **34** 163–4
[33] Schrödinger E 1999 About Heisenberg uncertainty relation (arXiv:quant-ph/9903100)
[34] Yunger Halpern N, Swingle B and Dressel J 2018 Quasiprobability behind the out-of-time-ordered correlator *Phys. Rev. A* **97** 042105
[35] Arvidsson-Shukur D R M, Chevalier Drori J and Yunger Halpern N 2021 Conditions tighter than noncommutation needed for nonclassicality *J. Phys. A: Math. Theor.* **54** 284001
[36] De Bièvre S 2021 Complete incompatibility, support uncertainty and Kirkwood–Dirac nonclassicality *Phys. Rev. Lett.* **127** 190404
[37] Santini A, Solfanelli A, Gherardini S and Collura M 2023 Work statistics, quantum signatures and enhanced work extraction in quadratic fermionic models *Phys. Rev. B* **108** 104308
[38] Budiyono A and Dipojono H K 2023 Quantifying quantum coherence via Kirkwood–Dirac quasiprobability *Phys. Rev. A* **107** 022408
[39] Wagner R, Schwartzman-Nowik Z, Paiva I L, Te'eni A, Ruiz-Molero A, Barbosa R S, Cohen E and Galvão E F 2024 Quantum circuits for measuring weak values, Kirkwood–Dirac quasiprobability distributions and state spectra *Quantum Sci. Technol.* **9** 015030
[40] Arvidsson-Shukur D R M, Braasch W F Jr, De Bievre S, Dressel J, Jordan A N, Langrenez C, Lostaglio M, Lundeen J S and Yunger Halpern N 2024 Properties and applications of the Kirkwood–Dirac distribution *New J. Phys.* **26** 121201
[41] Johansen L M 2007 Quantum theory of successive projective measurements *Phys. Rev. A* **76** 012119
[42] Gherardini S and De Chiara G 2024 Quasiprobabilities in quantum thermodynamics and many-body systems *PRX Quantum* **5** 030201
[43] Spekkens R W 2008 Negativity and contextuality are equivalent notions of nonclassicality *Phys. Rev. Lett.* **101** 020401
[44] Hofmann H F 2012 How weak values emerge in joint measurements on cloned quantum systems *Phys. Rev. Lett.* **109** 020408
[45] Pusey M F 2014 Anomalous weak values are proofs of contextuality *Phys. Rev. Lett.* **113** 200401
[46] Dressel J, Malik M, Miatto F M, Jordan A N and Boyd R W 2014 *Colloquium*: understanding quantum weak values: basics and applications *Rev. Mod. Phys.* **86** 307–16
[47] Hofer P P 2017 Quasi-probability distributions for observables in dynamic systems *Quantum* **1** 32
[48] Kunjwal R, Lostaglio M and Pusey M F 2019 Anomalous weak values and contextuality: robustness, tightness and imaginary parts *Phys. Rev. A* **100** 042116
[49] Schmid D, Baldijão R D, Yı Y, Wagner R and Selby J H 2024 Kirkwood–Dirac representations beyond quantum states and their relation to noncontextuality *Phys. Rev. A* **110** 052206
[50] Schmid D, Selby J H, Pusey M F and Spekkens R W 2024 A structure theorem for generalized-noncontextual ontological models *Quantum* **8** 1283
[51] Piacentini F *et al* 2016 Experiment investigating the connection between weak values and contextuality *Phys. Rev. Lett.* **116** 180401
[52] Piacentini F *et al* 2016 Measuring incompatible observables by exploiting sequential weak values *Phys. Rev. Lett.* **117** 170402
[53] Cimini V, Gianani I, Piacentini F, Degiovanni I P and Barbieri M 2020 Anomalous values, Fisher information and contextuality, in generalized quantum measurements *Quantum Sci. Technol.* **5** 025007
[54] Lupu-Gladstein N, Yilmaz Y B, Arvidsson-Shukur D R M, Brodutch A, Pang A O T, Steinberg A M and Halpern N Y 2022 Negative quasiprobabilities enhance phase estimation in quantum-optics experiment *Phys. Rev. Lett.* **128** 220504

[55] Hernández-Gómez S, Isogawa T, Belenchia A, Levy A, Fabbri N, Gherardini S and Cappellaro P 2024 Interferometry of quantum correlation functions to access quasiprobability distribution of work *npj Quantum Inf.* **10** 115
[56] Shrimali D, Panda B and Pati A K 2024 Stronger speed limit for observables: tighter bound for the capacity of entanglement, the modular Hamiltonian and the charging of a quantum battery *Phys. Rev. A* **110** 022425
[57] Veitch V, Ferrie C, Gross D and Emerson J 2012 Negative quasi-probability as a resource for quantum computation *New J. Phys.* **14** 113011
[58] Gardas B and Deffner S 2018 Quantum fluctuation theorem for error diagnostics in quantum annealers *Sci. Rep.* **8** 17191
[59] Buffoni L and Campisi M 2020 Thermodynamics of a quantum annealer *Quantum Sci. Technol.* **5** 035013
[60] Cimini V, Gherardini S, Barbieri M, Gianani I, Sbroscia M, Buffoni L, Paternostro M and Caruso F 2020 Experimental characterization of the energetics of quantum logic gates *npj Quantum Inf.* **6** 96
[61] Deffner S 2021 Energetic cost of Hamiltonian quantum gates *Europhys. Lett.* **134** 40002
[62] Buffoni L, Gherardini S, Zambrini Cruzeiro E and Omar Y 2022 Third law of thermodynamics and the scaling of quantum computers *Phys. Rev. Lett.* **129** 150602
[63] Stevens J *et al* 2022 Energetics of a single qubit gate *Phys. Rev. Lett.* **129** 110601
[64] Aifer M and Deffner S 2022 From quantum speed limits to energy-efficient quantum gates *New J. Phys.* **24** 055002
[65] Gianani I, Belenchia A, Gherardini S, Berardi V, Barbieri M and Paternostro M 2023 Diagnostics of quantum-gate coherences deteriorated by unitary errors via end-point-measurement statistics *Quantum Sci. Technol.* **8** 045018
[66] Śmierzchalski T, Mzaouali Z, Deffner S and Gardas B 2024 Efficiency optimization in quantum computing: balancing thermodynamics and computational performance *Sci. Rep.* **14** 4555
[67] Aifer M, Myers N M and Deffner S 2023 Thermodynamics of quantum information in noisy polarizers *PRX Quantum* **4** 020343
[68] Aifer M, Thingna J and Deffner S 2024 Energetic cost for speedy synchronization in non-Hermitian quantum dynamics *Phys. Rev. Lett.* **133** 020401
[69] Perarnau-Llobet M, Bäumer E, Hovhannisyan K V, Huber M and Acin A 2017 No-go theorem for the characterization of work fluctuations in coherent quantum systems *Phys. Rev. Lett.* **118** 070601
[70] Campisi M, Hänggi P and Talkner P 2011 *Colloquium*: quantum fluctuation relations: foundations and applications *Rev. Mod. Phys.* **83** 771–91
[71] Halliwell J J 2016 Leggett–Garg inequalities and no-signaling in time: a quasiprobability approach *Phys. Rev. A* **93** 022123
[72] Pei J-H, Chen J-F and Quan H T 2023 Exploring quasiprobability approaches to quantum work in the presence of initial coherence: advantages of the Margenau-Hill distribution *Phys. Rev. E* **108** 054109
[73] He J and Fu S 2024 Nonclassicality of the Kirkwood–Dirac quasiprobability distribution via quantum modification terms *Phys. Rev. A* **109** 012215
[74] García-Pintos L P, Nicholson S B, Green J R, Campo A and Gorshkov A V 2022 Unifying quantum and classical speed limits on observables *Phys. Rev. X* **12** 011038
[75] Nicholson S B, García-Pintos L P, Campo A and Green J R 2020 Time–information uncertainty relations in thermodynamics *Nat. Phys.* **16** 1211–5
[76] Touil A, Çakmak B and Deffner S 2021 Ergotropy from quantum and classical correlations *J. Phys. A: Math. Theor.* **55** 025301
[77] Pusz W and Woronowicz S L 1978 Passive states and KMS states for general quantum systems *Commun. Math. Phys.* **58** 273–90
[78] Alicki R 1979 The quantum open system as a model of the heat engine *J. Phys. A: Math. Gen.* **12** L103
[79] Uzdin R, Levy A and Kosloff R 2015 Equivalence of quantum heat machines and quantum-thermodynamic signatures *Phys. Rev. X* **5** 031044
[80] Myers N M, Abah O and Deffner S 2022 Quantum thermodynamic devices: from theoretical proposals to experimental reality *AVS Quantum Sci.* **4** 027101
[81] Cangemi L M, Bhadra C and Levy A 2024 Quantum engines and refrigerators *Phys. Rep.* **1087** 1–71
[82] Campaioli F, Gherardini S, Quach J Q, Polini M and Andolina G M 2024 *Colloquium*: quantum batteries *Rev. Mod. Phys.* **96** 031001
[83] Fedorov A K, Gisin N, Beloussov S M and Lvovsky A I 2022 Quantum computing at the quantum advantage threshold: a down-to-business review (arXiv:2203.17181)